International Journal of Civil and Structural Engineering– IJCSE
Volume 3 : Issue 1 *[ISSN : 2372-3971]*

Publication Date: 18 April, 2016

Shear Locking in Bilinear Quadratic Plane Elements

[Shokry A. & Spiliopoulos K.V.]

***Abstract*— In Finite Element Analysis, unlike the classical beam theory, when a beam is modeled using Q4 (Bilinear Quadratic) plane element, the bending moment appears to be less than that of the exact one, i.e. the normal stresses are less than their exact values. The difference between the results of the bending moment indicates that the beam is more stiffened. This problem is defined as shear locking. It is related to the linear representation of the displacement field of that plane element. There are several methods to eliminate the shear locking effect either by increasing the mesh size of the elements, using elements with more nodes, or using numerical integration to integrate the stiffness matrix. Each of the mentioned methods are applied on a cantilever beam modeled using MATLAB.**

***Keywords*— Shear locking; FEM (Finite Element Method); Q4 elements (Bilinear Quadrilateral elements); Q6 elements (Improved Bilinear Quadrilateral elements); Gauss Quadrature**

I. Introduction

Generally, locking effect is used by engineers to describe the case where the FE (Finite Element) computations produce smaller displacements than it should be. It also could be defined as the excessive stiffness in one or more deformation mode [3] [7].

Q4 element cannot model pure bending moment. Shear strain appears (which should not have appeared) as well as the bending strain, so the bending moment appears to be less than the expected value.

Many researches have worked to solve the shear locking problem. In 1973, E. L. Wilson et al. published in “Incompatible Displacement Methods” a new element to treat the defects in the Q4 element, the improved bilinear Quadrilateral Element Q6. This new element succeeded to get better results in more efficient and simple way. However, some defects appeared in this element that could be treated by using good mesh refinement.

Also, using different numerical integration to integrate the global stiffness matrix, is a good solution to reduce the over-stiffness behavior of the beam. These methods of integration approach the exact results with almost no defects. This could be achieved using Gauss quadrature integration. However, an insufficient choice of Gauss points may cause a spurious mode which has a really bad effect on the deformation of the element.

Shokry A.

Lecturer Assistant in Civil Engineering department, Faculty of Engineering and Material Sciences, the German University in Cairo, Egypt

Spiliopoulos K. V.

Professor in Structural Mechanics, Department of Civil Engineering, National Technical University of Athens, Greece

This paper aims to model the treatment of the locking problem and to analyze and detect the deficiency of each of them. A FE analysis of a cantilever beam is done using 3 different meshing sizes. MATLAB is used to model and analyze the beam.

II. Problem Definition

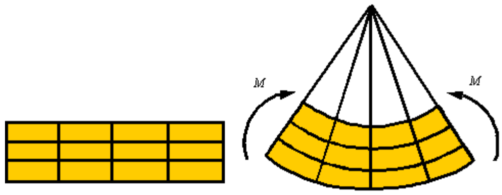

Figure 1. Pure Bending **[10]**

In the classical beam theory (Bernoulli’s beam), there are two important assumptions. First, the contribution of the shear deformation is negligible compared to the rotation; this is equivalent to consider the plane sections of the beam - normal to the longitudinal axes- plane and perpendicular to the new Neutral Axes while the top and bottom edges of the beam become arcs of the same curvature (as described in the deformed shape of the beam subjected to pure bending in Fig. 1). The second assumption is that the thickness of the beam should be small compared to the other dimensions [1] [4].

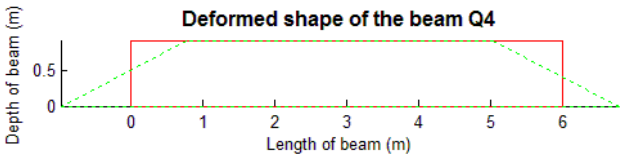

Figure 2. Deformed shape of a simple beam subjected to pure bending

$$u = \beta_1 + \beta_2 x + \beta_3 y + \beta_4 xy \qquad (1)$$

$$v = \beta_5 + \beta_6 x + \beta_7 y + \beta_8 xy \qquad (2)$$

$$\varepsilon_x = \beta_2 + \beta_4 y \qquad (3)$$

$$\varepsilon_y = \beta_7 + \beta_8 x \qquad (4)$$

$$\gamma_{xy} = (\beta_3 + \beta_6) + \beta_4 x + \beta_8 y \qquad (5)$$

Fig. 2 shows a simple beam -modeled using Q4 element- subjected to pure bending. Unlike the classical beam theory, the edges of the beam are inclined having an acute angle with the Neutral axis; as a result of the displacement field of Q4 element in Equation (1) & (2). This acute angle is a sign of development of shear strains (strain field are shown in Equation (3), (4) & (5)) and consequently shear stresses. The developed shear stresses that develop lead to over-stiffness in the beam element; that is, the bending moment is resisted by both flexure and shearing stresses.

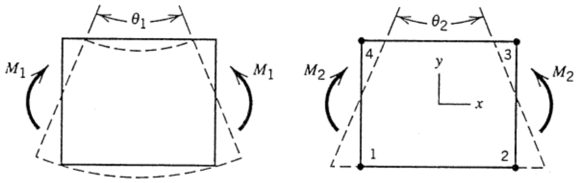

Figure 3 Pure bending and bending in Q4 element [4]

$$M_2 = \frac{1}{1+\nu}\left[\frac{1}{1-\nu}+\frac{1}{2}\left(\frac{a}{b}\right)^2\right]M_1 \quad (6)\ [4]$$

Another approach to define the shear locking could be explained as follows. The two beams in Fig. 3 have the same properties (Poisson's ratio, elasticity…etc.). Apply moments in each beam (M_1 and M_2) to get equal angles (θ_1 and θ_2). Equation (6) shows the relation between the two bending moments where a/b is the aspect ratio (α is the length of the beam and b is the height). If the aspect ratio increases so much which means insufficient mesh refinement (as shown in Fig. 2, where the beam under pure bending is modeled by only one element) the moment of the Q4 element will increase so much compared to the exact one, in other meaning, the element becomes infinitely stiff in bending and this phenomena is called *locking*. Practically, this large aspect ratio is avoided by good mesh refinement (as shown in the analysis of the Q4 element later) [4].

Two remedies are discussed to solve this problem. The first remedy is supplementing the element with additional modes to allow some flexibility to the element. The second remedy is using reduced integration methods to integrate the global stiffness matrix K.

III. FE analysis

Three Cantilever beams are modeled using different meshing sizes by MATLAB. The first one is analyzed with only 6 elements, the second one with 60 elements while the third one is divided to 1080 elements. Each beam has a length of 6 m, the height is 0.9 m and while its thickness is 0.3 m. The modulus of Elasticity of its material is $210*10^6$ KN/m^2 and its Poisson's ratio is 0.3. They are loaded by 50 KN at the free end divided in the two nodes, each of 25 KN.

According to the classical beam theory [1], the maximum normal stress is 7404 KN/m^2 and the deflection is $9.406*10^{-4}$ m as shown in Equation (7) & (8) receptively.

$$\sigma_x = \frac{M_x y}{I_x} \quad (7)$$

$$v = \frac{-P_y L^3}{3EI_x} \quad (8)$$

The deformed shape of the beam shown in Fig. 4 clarifies the linear relation of the displacement field and x & y (Equation (1) & (2)). It also shows that ε_x is independent of x (ε_x is constant along the length of the beam); which means that Q4 cannot model a state of pure bending.

The FE analysis shows that the maximum normal stress using 6 Q4 elements is 2110 KN/m^2 which is too small compared to the exact value 7407 KN/m^2. While the shear stress[1] shown in Fig. 5a for the same model is -731 KN/m^2 which is too large compared to the corresponding exact value -277.7 KN/m^2. By increasing the meshing size, the deflection and the normal stress reach $-8.449*10^{-4}$ m and 4831 KN/m^2 respectively, while the shear stress approaches its exact value which is zero[2]. So, it is obvious that the normal stress of the FE model -in small mesh size- is less than that of the exact value, while the shear stress is more than the exact value as a result of the shear locking problem.

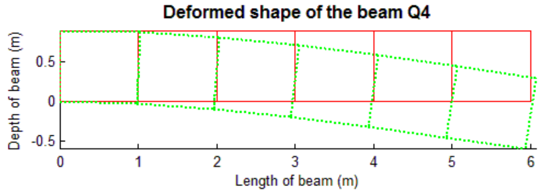

Figure 4 Deformation of Cantilever beam- 6 elements using Q4 element

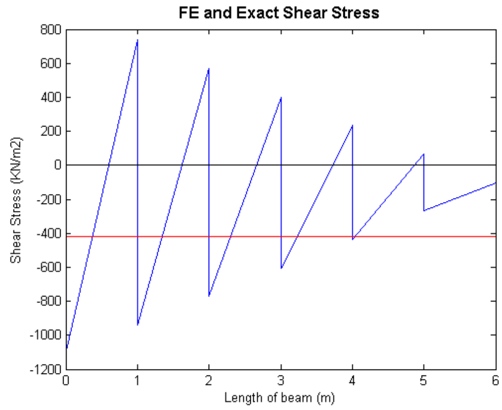

(a) [8][3]

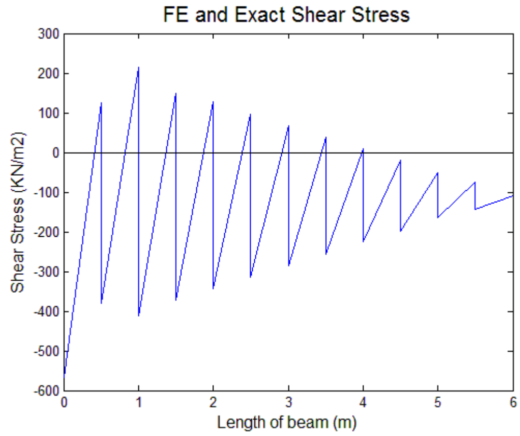

(b)

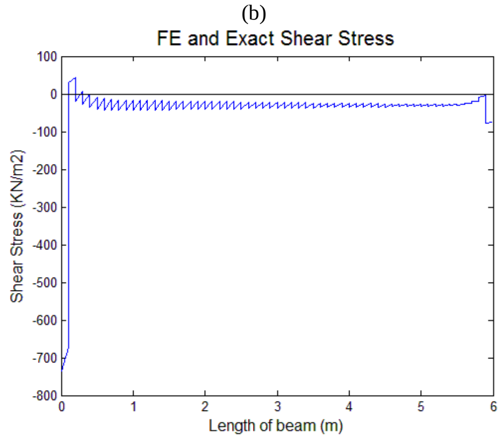

(c)

Figure 5 Analysis of Cantilever Beam - 1080 elements using Q4 element

[1] The shear stress in Fig. 4a was calculated at the centroid of the elements.

[2] The shear stress in Fig. 4b & 4c was calculated at the top elements.

[3] The MATLAB code in the reference mentioned was modified.

International Journal of Civil and Structural Engineering– IJCSE
Volume 3 : Issue 1 [ISSN : 2372-3971]

Publication Date: 18 April, 2016

IV. Improved Bilinear Quadrilateral Element Q6

$$u = \sum_{i=1}^{4} N_i u_i + (1-\xi^2)\alpha_1 + (1-\eta^2)\alpha_2 \qquad (9)$$

$$v = \sum_{i=1}^{4} N_i v_i + (1-\xi^2)\alpha_3 + (1-\eta^2)\alpha_4 \qquad (10)$$

Incompatible elements or Improved Q4 element have been developed with six shape functions as shown in Equation (9) & (10); where α_i are the generalized coordinates. The two additional displacement modes shown in Fig. 6 allow some flexibility in the beam and satisfy the pure bending conditions. They are also called as nodeless d.o.f. (Degrees of freedom). The additional displacement modes accompanied by them are called incompatible displacement fields because they allow overlaps or gaps between the elements; each element has its own nodeless d.o.f. and they are not connected to each other.

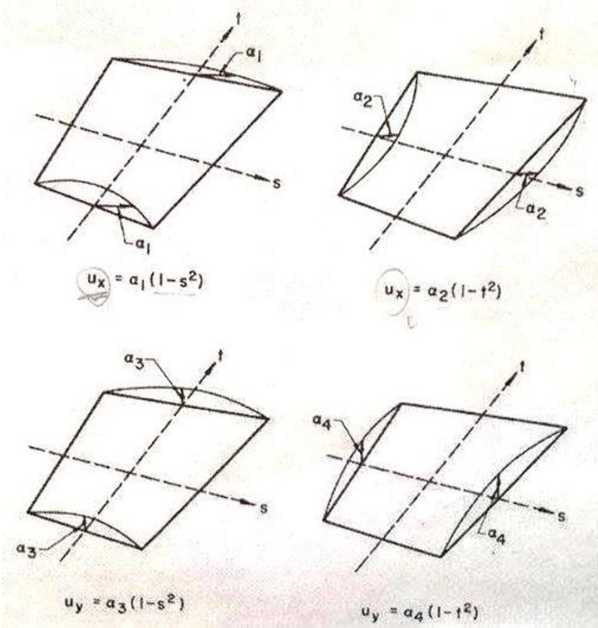

Figure 6 Additional displacement modes [2]

$$\{\varepsilon\} = [B_c][B_I]\begin{Bmatrix} d_c \\ d_I \end{Bmatrix} \qquad (11)$$

$$[B] = [B_c][B_i] \qquad (12)$$

$$[B_c] = \frac{1}{|J|}[\Gamma]\begin{bmatrix} N_{1,\xi} & 0 & N_{2,\xi} & 0 & N_{3,\xi} & 0 & N_{4,\xi} & 0 \\ N_{1,\eta} & 0 & N_{2,\eta} & 0 & N_{3,\eta} & 0 & N_{4,\eta} & 0 \\ 0 & N_{1,\xi} & 0 & N_{2,\xi} & 0 & N_{3,\xi} & 0 & N_{4,\xi} \\ 0 & N_{1,\xi} & 0 & N_{2,\eta} & 0 & N_{3,\eta} & 0 & N_{4,\eta} \end{bmatrix} \qquad (13)$$

$$; \text{where } [\Gamma] = \begin{bmatrix} J_{22} & -J_{12} & 0 & 0 \\ 0 & 0 & -J_{21} & J_{11} \\ -J_{21} & J_{11} & J_{22} & -J_{12} \end{bmatrix}$$

$$[B_I] = \frac{1}{|J|}[\Gamma]\begin{bmatrix} -2\xi & 0 & 0 & 0 \\ 0 & -2\eta & 0 & 0 \\ 0 & 0 & -2\xi & 0 \\ 0 & 0 & 0 & -2\eta \end{bmatrix} \qquad (14)$$

$$K_{CC_{8\times8}} = t\int_{-1}^{1}[B_c]^T_{8\times3}[E]_{3\times3}[B_c]_{3\times8}|J|\,d\xi d\eta \qquad (15)$$

$$K_{CI_{8\times4}} = t\int_{-1}^{1}[B_c]^T_{8\times3}[E]_{3\times3}[B_I]_{3\times4}|J|\,d\xi d\eta \qquad (16)$$

$$K_{IC_{4\times8}} = t\int_{-1}^{1}[B_I]^T_{4\times3}[E]_{3\times3}[B_c]_{3\times8}|J|\,d\xi d\eta \qquad (17)$$

$$K_{II_{4\times4}} = t\int_{-1}^{1}[B_I]^T_{4\times3}[E][B_I]_{3\times4}|J|\,d\xi d\eta \qquad (18)$$

$$K_{12\times12} = \begin{bmatrix} K_{CC} & K_{CI} \\ K_{IC} & K_{II} \end{bmatrix} \qquad (19)$$

$$\{d_c\} = [u_1 \quad v_1 \quad u_2 \quad v_2 \quad u_3 \quad v_3 \quad u_4 \quad v_4]^T \qquad (20)$$

$$\{d_I\} = [u_5 \quad u_6 \quad v_5 \quad v_6]^T \qquad (21)$$

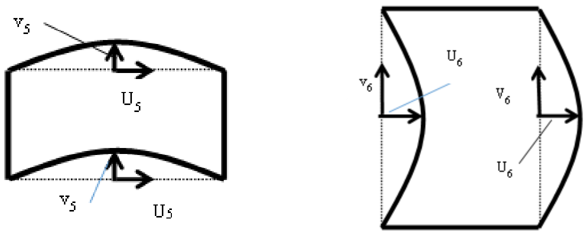

(a) (b)

Figure. 7 Displacement modes of Q6 element

The strain of Q6 element in Equation (11) consists of the strain of the nodal d.o.f and that of the nodeless d.o.f. In Equation (12), the deformation matrix [B] for this element is expanded to include the deformation matrix of the compatible displacements of Q4 element $[B_c]$ and that of the additional incompatible displacements $[B_i]$. $[B_c]$ in Equation (13) is the same as calculated before in Q4 element. The Jacobian matrix is based only on the nodal d.o.f, so it is not changed. The incompatible displacement field is added to the shape function matrix and its deformation matrix can be found as in Equation (14). The stiffness matrix of a Q6 element in Equation (19) consists of four matrices explained in Equation (15) to (18). The displacement mode of Equation (21) is shown in Fig. 7 [5] [7].

A. *Defects of the Q6 element*

However, the Q6 element in this way fails to represent a state of constant stress unless it is rectangular. Consider a mesh of non-rectangular elements is loaded in a way to prevail a state of constant stress, in case of absence of nodeless d.o.f (Q4 element), the elements will behave properly. But in case of the presence of the nodeless d.o.f., the elements will not respond properly. The nodeless d.o.f. should be zeros but they are not.

A remedy for this defect is adding initial stresses vector $\{\sigma_0\}$ to represent the state of uniform stresses. By applying uniform stresses, zeros nodeless d.o.f could be achieved by doing a patch test as Equation (22) shows. To satisfy this patch test, the deformation matrix of the incompatible d.o.f. should be modified by adding a corrected deformation matrix as Equation (23) shows. The corrected deformation matrix $[B_{i\ corr}]$ in Equation (27) is solved by substituting Equation (23) in Equation (22) [5] [7].

$$\int [B_i]^T\{\sigma_0\}\,dV = \{0\}, \quad \text{hence} \int [B_i]^T\,dV = \{0\} \tag{22}$$

$$[B_{i\ new}] = [B_i] + [B_{i\ corr}] \tag{23}$$

$$\int [B_{i\ new}]^T\,dV = \{0\} \tag{24}$$

$$\int ([B_i] + [B_{i\ corr}])\,dV = \{0\} \tag{25}$$

$$\int [B_i]\,dV + V[B_{i\ corr}] = \{0\} \tag{26}$$

$$[B_{i\ corr}] = \frac{-1}{V}\int [B_i]dV \tag{27}$$

Another defect of the Q6 element is incompatibility between elements. The nodeless d.o.f. (α_1 to α_4) are not connected between the elements except for the nodal d.o.f. This may allow some gaps or overlaps between the elements as shown in Fig. 8. However, this defect could be avoided by good mesh refinement [4].

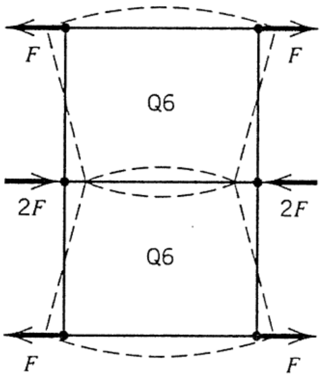

Figure 8 Incompatibility modes in Q6 element [4]

B. *Illustrative example*

TABLE I Results of Q4 & Q6 elements

	Elements	Exact	Q4 element	Q6 element
Normal stress (KN/m^2)	6	7407	2110	3056
	60		4831	5848
	1080		6637	6611
Deflection (m)	6	-9.406*10^{-4}	-6.078*10^{-4}	-9.36*10^{-4}
	60		-8.449*10^{-4}	-8.9*10^{-4}
	1080		-9.49*10^{-4}	-9.5*10^{-4}

The cantilever beam in the previous examples is now modeled by the Q6 element. Table I shows that the values of the maximum deformation and normal stresses are improved and approaching the exact values rather than that of Q4 element as a result of reducing the shear locking problem. So the beam now in Q6 element is not over-stiffened in bending. Also Fig.9 shows better results of the shear stresses compared to its corresponding in Q4 element.

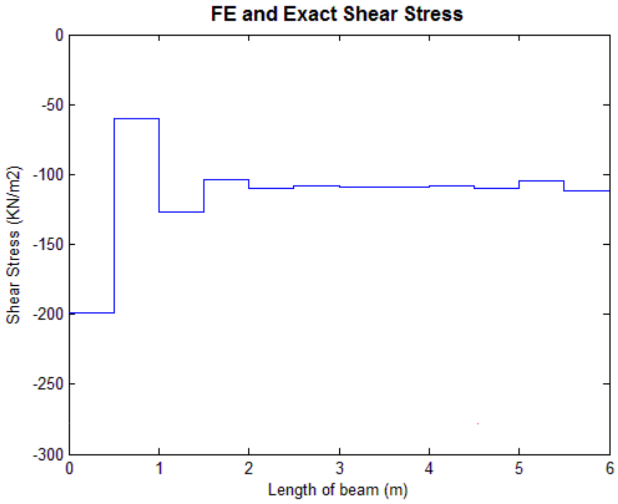

Figure 9 Analysis of Cantilever Beam – 60 elements using Q6 element

V. Weighted Integration method

Comparing the exact strain energy of the element to that modeled by FEA (Finite Element Analysis) is a way to know whether the element is over-stiffened or not. The energy ratio r in Equation (28) shows the relation between the strain energy of Q4 element U_{quad} and the exact one of the beam U_{beam}. If it is greater than 1, then the element is over-stiffened, but if it is less than 1, it is under-stiffened, and the result is exact if it is equal to 1 [6].

$$r = \frac{U_{quad}}{U_{beam}} \tag{28}$$

$$U_{quad} = \frac{1}{2}[u_{beam}]^T[K^e]\{u_{beam}\} \tag{29}$$

$$U_{beam} = \frac{1}{2}M\kappa a = \frac{M^2 a}{2EI} = \frac{6M^2}{Eha^2\gamma^3} \tag{30}$$

$$r = \frac{1 - \frac{2}{\gamma^2} - v}{\left(\frac{2}{\gamma^2}\right)(1 - v^2)} \tag{31}$$

[6]

It is required to find a value of r in terms of the element dimension. Consider a beam subjected to pure bending and is divided to Q4 element each of length α and height b. The strain energy in the Q4 elements is computed as in Equation (29), where u_{beam} is the nodal displacement vector and consists of u_x & u_y, and K^e is the stiffness matrix of the element. But $K^e \times u_y$ vanishes because this is a state of pure bending and no shear forces are developed. The corresponding strain energy in this beam segment is calculated using Equation (30), where M is the applied bending moment and κ is the curvature of the beam.

The energy ratio r can be calculated in terms of the aspect ratio γ (b/a) and Poisson's ratio ν by substituting both of Equation (29) & Equation (30) in Equation (28). From Equation (31), if γ is much larger than 1, r will be much smaller than 1 and the element is under-stiffened and vice versa. This is similar to what it had been discussed before, in the first section, specifically in Equation (6). High values of r cause shear locking problems.

A remedy for this problem is to compensate the difference in the energy ratio by getting an adjusted stiffness matrix integrated by the weighted integration method. It is better to get the stiffness matrix of an element by using a linear combination of stiffness produced by two different integration rules and this is called weighted integration method. Equation (32) shows the stiffness matrix of a 4-node element formulated by combining two stiffness matrices integrated by 1×1 and 2×2 gauss points, while β is a factor to reduce the shear locking effect (Equation (33) & (34)). In the linear combination of Equation (32), $K_{1\times1}$ is too soft and $K_{2\times2}$ is too stiff. Such a combination may give balanced stiffness to adjust the energy ratio, as mentioned.

$$K_{\beta}^{e} = (1-\beta)K_{1\times1}^{e} + \beta K_{2\times2}^{e} \quad (32)$$

$$r = \frac{\beta\left(1-\frac{2}{\gamma^2}-v\right)}{\left(\frac{2}{\gamma^2}\right)(1-v^2)} \quad (33)$$

$$\beta = \frac{\left(\frac{2}{\gamma^2}\right)(1-v^2)}{\left(1-\frac{2}{\gamma^2}-v\right)} \quad (34)$$

A. *Illustrative Example*

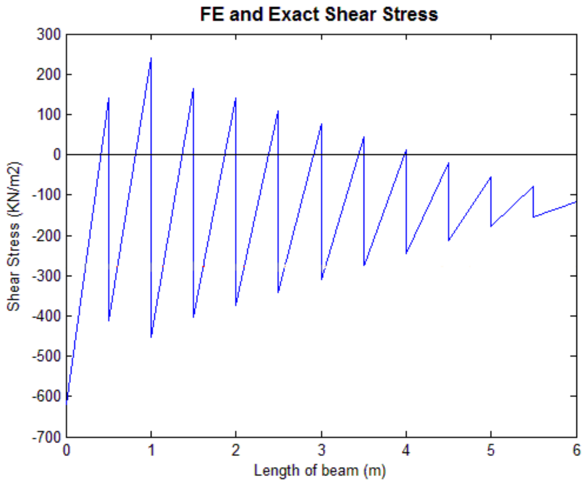

Figure 10 Analysis of Cantilever Beam – 60 elements using Q4 element with Weighted Integration method

The same cantilever used before is now modeled using the weighted integration method. Table II shows better results compared to Q4 elements (without weighted integration method) in both deformation and normal stresses as a result of some reduction in the shear locking problem. The shear stresses in Fig.10 are almost the same compared to its corresponding in Q4 elements (without weighted integration method).

TABLE II Results of the Q4 using Weighted Int. Method

	Elements	Exact	Q4 element	Weighted Int.
Normal stress (KN/m^2)	6	7407	2110	2977
	60		4831	5514
	1080		6637	7228
Deflection (m)	6	$-9.406*10^{-4}$	$-6.078*10^{-4}$	$-8.54*10^{-4}$
	60		$-8.449*10^{-4}$	$-9.26*10^{-4}$
	1080		$-9.49*10^{-4}$	-0.001

Concluding remarks

Fig. 11 summarizes the results of the analysis presented in this work. It shows a comparison of the different types of elements and procedures that were used. The small values of the normal stresses of Q4 element is a result of the shear locking problem. This problem is reduced using Q6 element, by adding two additional displacement modes. Another remedy to the problem is done by splitting the stiffness matrix (or the elasticity matrix) to two parts where each part is integrated separately using different Gauss points.

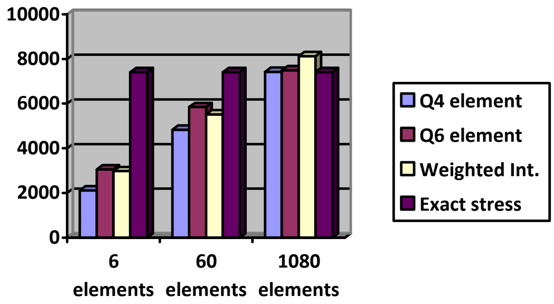

Figure 11 Comparison of the different elements with respect to the max. Normal stresses

Acknowledgment

I would like to express my gratitude to Prof. Spiliopoulos in supporting me with the materials to work on this paper.

References

[1]	A. E. Armenakas, Advanced Mechanics of Materials and Applied Elasiticity, CRC Press, 2005.
[2]	E. L. Wilson, L. R. Taylor, W. P. Doherty and J. Ghaboussi, "Incompatible Displacement Models," *Numerical and Computer Methods in Structural Mechanics*, pp. 43-57, 1973.
[3]	D. Braess, Finite elements: theory fast solvers and applications in solid mechanics, 2nd ed., Bochum: Springer Verlag, 1992.
[4]	R. D. Cook, Finite Element Modeling For Stress Analysis, 1st ed., Madison: John Wiley & Sons, Inc., 1994, p. 1.
[5]	E. L. Wilson, "Ed Wilson Website," [Online]. Available: http://www.edwilson.org/BOOK-Wilson/06-incom.pdf. [Accessed 17 June 2014].
[6]	C. A. Felippa, "Introduction to Finite Element Methods," 2004. [Online]. Available: http://www.colorado.edu/engineering/cas/courses.d/IFEM.d/IFEM.Ch00.d/IFEM.Ch00.pdf. [Accessed 13 April 2014].
[7]	R. D. Cook, D. S. Malkus, M. E. Plesha and R. J. Witt, Concepts and applications of finite element analysis, 4th ed., Madison: John Wiley & Sons. Inc., 2002.
[8]	P. I. Kattan, MATALB Guide to Finite Elements, 2nd ed., Amman: Springer, 2006.
[9]	A. E. Armenakas, Advanced Mechanics of Materials And Applied Elasticity, CRC Press, 2005.
[10]	U. o. N. Department of Engineering Mechanics, "Pure Bending," 1996. [Online]. Available: http://emweb.unl.edu/NEGAHBAN/Em325/11-Bending/Bending.htm. [Accessed 30 May 2014].